Cathodoluminescence of conducting gratings and implications for electron-beam investigations of nano-photonic devices

Janardan Nath[a], Casey Schwarz[a], Evan Smith[a], Chandana Ghosh[a], R. E. Peale[a], L. Chernyak[a], Walter R. Buchwald[b]

[a]Department of Physics, University of Central Florida, Orlando FL 32816

[b]Solid State Scientific Corporation, 27-2 Wright Road, Hollis, NH 03049

ABSTRACT

Cathodoluminescence (CL) spectroscopy is performed on conducting 1- and 2-dimensional gratings of metals, semi-metals and semi-conductors of varying periods from 0.5 to 20 microns for a range of grating amplitudes from 0.1 to 4.6 microns. The overall emission spectrum consists of a 400 nm wide band centered at ~600 nm which depends little on the grating period, grating amplitude, material, e-beam energy, or temperature. CL intensity increases and the center wavelength blue shifts with increasing excitation beam current. For the larger amplitude 1-dimensional gratings fringes appear in the emission spectrum, which is due to interference between emission from grating bars and grooves. Surface corrugation is necessary to the emission as none is observed from smooth surfaces. The same band appears weakly in CL of a Cu sample with random ~1 micron surface roughness, but this emission is strongly reduced when the same sample is highly polished. The CL signal appears even when the ~10 nm electron-beam is at least 2 mm away from the grating edge, suggesting electron-beam induced currents are important to the emission, whose precise mechanism remains unclear. Previously suggested mechanisms--electron collision with image charge, transition radiation, surface contamination, and inverse photoemission effect--all fail to explain the observed spectrum and its lack of beam-energy dependence.

Keywords: Cathodoluminescence, nano-photonics, Surface Plasmon Polaritons, transition radiation, inverse photoemission, plasmonics.

1. INTRODUCTION

Cathodoluminescence (CL) spectroscopy of structured metal surfaces has emerged recently as a means of studying the excitation and propagation of surface plasmon polaritons (SPP) [1, 2, 3, 4]. Such studies inform the design of future nano-photonic devices for sub-wavelength optics, data storage, light generation, solar cells, microscopy, and bio-photonics [5, 6]. However, the small fraction of the CL signal that can be attributed to SPPs typically rides on a substantial "background", whose thorough understanding is important for proper interpretation of SPP effects. This paper presents CL spectra that display interesting and substantial effects, which cannot be attributed to SPPs and which challenge some of the earlier interpretations.

Previous studies of SPPs by CL generally assume that SPPs and background emission are excited only within the 10 nm spot of a scanning electron microscope beam. It is further assumed that only the SPP component is able to propagate over distances of up to several microns to out-coupling structures, from which radiation is emitted and collected for spectral analysis. The propagation of the SPPs is found to depend on the type of metal surface studied and the wavelength: The characteristic propagation length differs for gold and silver[1,2,3] and increases with wavelength. In contrast, we find clear evidence that CL is emitted simultaneously over areas of at least several tens of microns diameter around the 10 nm e-beam spot. We studied metal, semimetal, and semiconductor surfaces, and the CL spectrum is found to be nearly the same for all of them. Surface corrugation appears necessary to obtain this characteristic CL signal. The signal strength and spectrum show little variation with the distance of the e-beam from an isolated grating structure up to distances of several mm, which greatly exceeds the characteristic SPP propagation lengths at optical frequencies, and hence rules out their participation in the signals we observe.

In agreement with previous studies [1, 2, 3, 4], we find that the bulk of the CL occurs in a band that is normally distributed around ~ 600 nm center wavelength. SPP effects should be revealed as a wavelength-dependent decrease in the signal as the excitation spot is removed from the edge of the out-coupling structure to distances up to several microns. Beyond this, the remaining signal would be "background", i.e. having no SPP contribution. The origin of this background has

been speculatively attributed to surface contamination[1], electronic transitions within the metal's band structure[1], collision of the impinging electrons with their image charges[1, 5], and transition radiation [5]. Inverse photo-electron effect[7] may also be added to the list of known CL emission processes for consideration. We show that none of these mechanisms can account for the observed spectrum. While a convincing explanation is yet lacking, we have made progress in experimentally constraining the possibilities.

2. THEORETICAL CONSIDERATIONS

Electrons incident on a metal surface are attracted and accelerated by their image charges, forming a set of accelerating dipoles that should radiate. This "collapsing dipole" has been suggested as explanation for the background CL[1,2,3]. The collision of an electron and its image is described by the motion of a particle with reduced mass $m/2$ in a hyperbolic trajectory with unity eccentricity. The total amount of energy radiated during the collision at frequency ω in the range $d\omega$ is given in this case by[9]

$$dE_\omega = \frac{\pi\omega^3 e^6}{6c^3E^2}[H_{iv}^{(1)'}(iv)]^2 d\omega = \frac{const\ \omega^3}{E^2}[H^{(1)}{}_{iv}(iv) - H^{(1)}{}_{iv+1}(iv)]^2 d\omega \quad (1)$$

where $E = mv_0^2/4$ is the total energy, $v = 2\omega e^2/mv_0^3$, v_0 is the initial electron velocity, and $H_{iv}^{(1)'}$ the derivative of the Hankel function $H^{(1)}{}_{iv}(iv)$ of the first kind of order iv. Eq. 1 gives no isolated band in the visible spectral range, and there is also expected to be a significant dependence on the electron energy.

Transition radiation occurs for uniform motion (without acceleration) of an electron passing from vacuum into any material. Equation (2) gives the transition radiation spectrum per unit solid angle, where n is the complex refractive index of the material, and θ is the emission angle relative to the surface normal[10]. The overall intensity of transition radiation depends quadratically on the initial electron velocity v_0.

$$\frac{dW_\omega}{d\Omega} = \frac{e^2 v_0{}^2}{\pi^2 c^3} sin^2\phi \left(\frac{(n^2-1)cos\phi}{n^2 cos\phi + \sqrt{n^2 - sin^2\phi}}\right)^2 \quad (2)$$

Fig. 1 presents calculated transition radiation integrated from -10 to 70 degrees (our experimental range of collection angle) for e-beam energies of 20 and 30 keV. This spectrum demonstrates the strong dependence of the radiation intensity on electron velocity. Furthermore, the spectrum demonstrates that transition radiation generally tends to concentrate at upper-visible and near UV wavelengths, with no isolated band appearing in the visible spectral range.

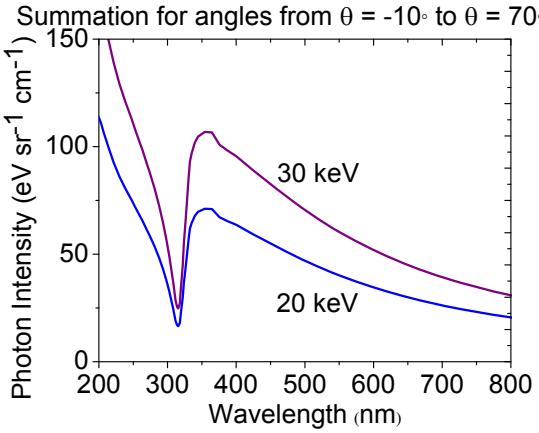

Fig. 1: Calculated spectrum of transition radiation integrated over collection angles -10 to 70 degrees for e-beam energy 20 and 30 keV.

Inverse photoemission is another mechanism of light emission when a metal is bombarded by energetic electrons. Inverse photoemission is generally very weak and occurs at UV wavelengths[7,8]. For Ag, Cu and Fe inverse photo-emission for normal incidence peaks around 270, 128, and 248 nm, respectively[7].

3. EXPERIMENTAL DETAILS

Lamellar gratings (period a = 7.5 or 20 micron, amplitude h = 0.1 to 4.6 micron) were photolithographically fabricated in silicon, in polyimide, or in photoresist. Optically-thick continuous coatings of Au, Ag, Sb and Bi were then deposited. Similar gratings were patterned on bare low resistivity silicon (0.1×10^{-3} and 8×10^{-3} Ω-cm, or 10^{21} and 10^{19} cm^{-3} carrier concentration). Grating profiles were measured using step or optical profilometers. Some gratings completely covered quarter sections of 2 inch wafers. For others, the structures were confined to 0.5 cm × 0.5 cm areas surrounded by smooth metal film. Even smaller gratings were fabricated by focused ion beam (FIB) milling in optically thick gold films (a = 500 nm or 1 micron, h = 100 nm amplitude, 10 or 30 periods). ProLIFT (Brewer Scientific), a spin-on co-developable polyimide, was used to create gratings with 20 micron period followed by gold coating. Fig. 2 presents optical microscope images of 1-dimensional and 2-dimensional gratings.

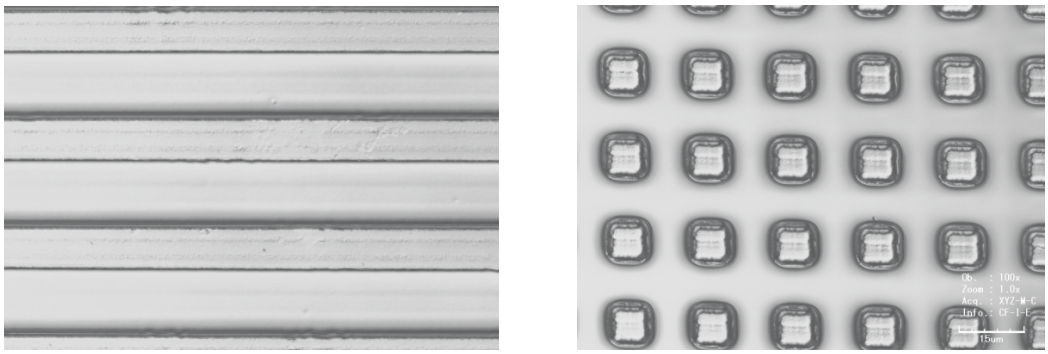

Fig. 2: Optical microscope images of 1-dimensional and 2-dimensional gold gratings.

CL was collected using a Gatan MonoCL3. Fig. 3 (left) presents a schematic of the CL excitation and collection geometry. The parabolic mirror collects the CL and sends it to the spectrometer through a light-guide. The closest distance between the mirror and the sample is 1 millimeter, which is the nominal focus position of the parabaloid. The electron beam energy was typically set to 20 keV, but it could be varied. The results were independent of the area over which the beam was rastered[11], the emission being essentially instantaneous in comparison to the e-beam residence time within any particular surface feature. For the small-area gratings, CL spectra were also collected with the electron beam outside the grating area, on surfaces of smooth unstructured metal, at various distances from the grating. Fig. 3 (right) shows that the number of grating bars that contribute to the collected CL signal depends on the distance z between sample and collection optic.

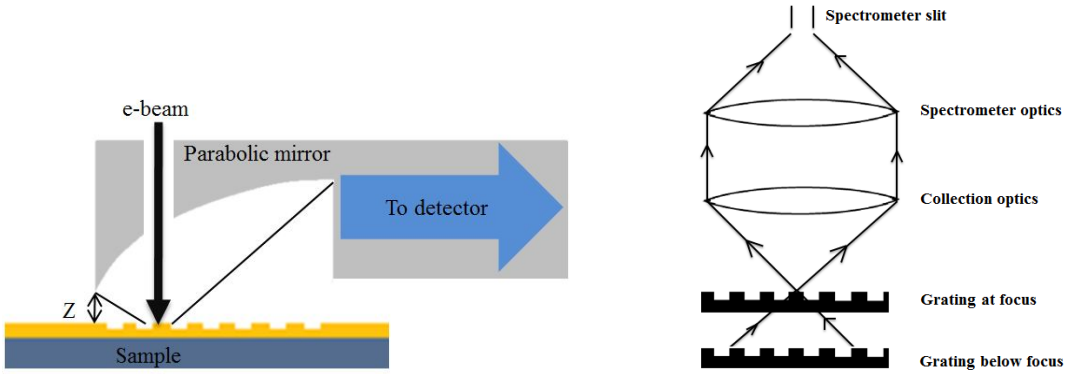

Fig. 3: (left) Schematic of SEM with CL collection paraboloid. (right) Schematic showing z-dependence of contributing sample area. (Lenses rather than the actual mirrors are shown for convenience.)

4. RESULTS

Fig. 4 (left) presents CL spectra for a = 20-micron Ag gratings of different h. The spectrally flat background level obtained when electron beam is blanked has been subtracted, curves have been normalized so that the peak has unity value, and the curves are offset vertically from each other for clarity. For small h, the emission band is smooth and featureless. For higher h, a periodic modulation appears whose period depends on grating amplitude and wavelength. The peak positions correspond to integral numbers of half wavelengths fitting into the depth of the grating grooves, i.e. $\lambda = 2h/m$ with m an integer. The triangle symbols indicate these positions.

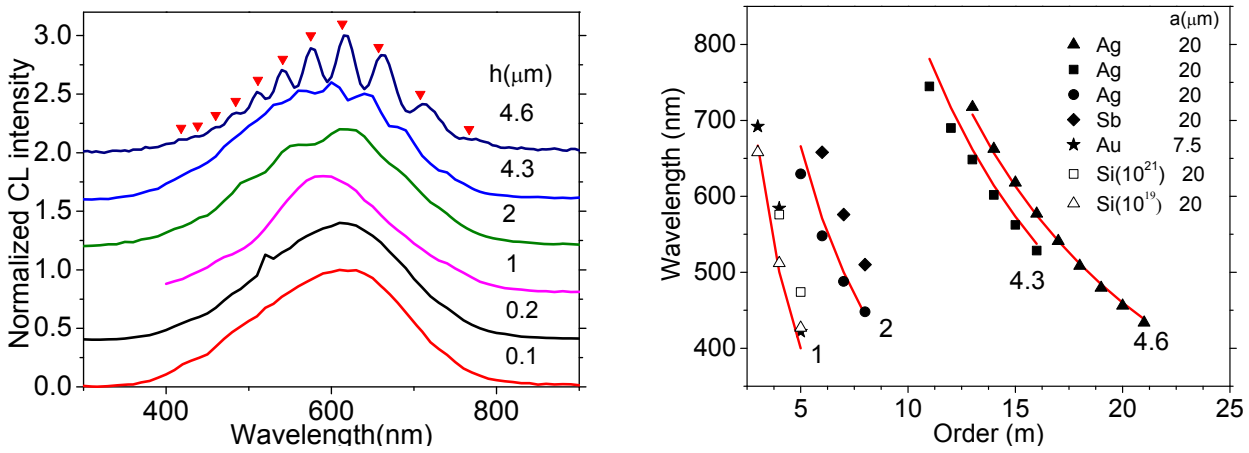

Fig. 4: (left) CL spectra for 20-micron-period Ag gratings of different amplitudes, with grating bars perpendicular to the optical collection axis, and (right) Modulation peak wavelength vs resonance order. Symbols are data and curves are calculated according to $\lambda = 2h/m$. The number at the bottom of each curve gives the grating amplitude h in microns.

Fig. 4 (right) presents the interference peak position vs. wavelength for these gratings made from different materials (metals, semimetals, and semiconductors) and with different grating periods and grating amplitudes. All of the different materials reveal the spectral oscillations, and the period of the oscillations appears to depend only on the grating amplitude. The modulation period increases with increasing wavelength and with decreasing grating amplitude. The data fit well to the curves $\lambda = 2h/m$, m = integer which confirms that the modulation is the effect of interference from emissions emanating simultaneously from grating bars and grooves. Since the period of the gratings is three orders larger than the e-beam spot size, the excitation volume for CL cannot be confined to the focused electron spot on the surface. Rather the excitation must be due to some far-propagating disturbance, such as an electron beam induced current of hot electrons.

Fig. 5 (left) presents example CL spectra for gratings made in different materials. The emission envelope, as well as the period of oscillations, does not depend on the material, nor do they depend on grating period. (Curiously, however, the amplitude of the oscillations in the semimetal Bi spectrum is zero, while the amplitude for the semimetal Sb is finite.) The main parameter affecting the period of the oscillations is the grating amplitude (Fig. 4, right). Independence of the spectral envelope on material argues against any mechanism that depends on electronic structure (interband transitions and inverse photoelectron effect) or permittivity (transition radiation).

Fig. 5 (right) presents CL spectra for different electron beam energies for silver gratings with a = 20 μm and h = 4.6 μm. The spectral envelop, intensity, and modulation features are all essentially independent of e-beam energy. This observation argues against any CL mechanism that depends on the initial electron velocity, such as collapsing dipole, transition radiation, or inverse photoelectron effect.

The visibility of the fringes is never 100%, but it always rides on an unmodulated background. The visibility does depend on the separation z of the sample and the CL collection parabola (Fig. 3). Fringe visibility is defined by,

$$Visibility = \frac{I_{max} - I_{min}}{I_{max} + I_{min}} \times 100 \qquad (3)$$

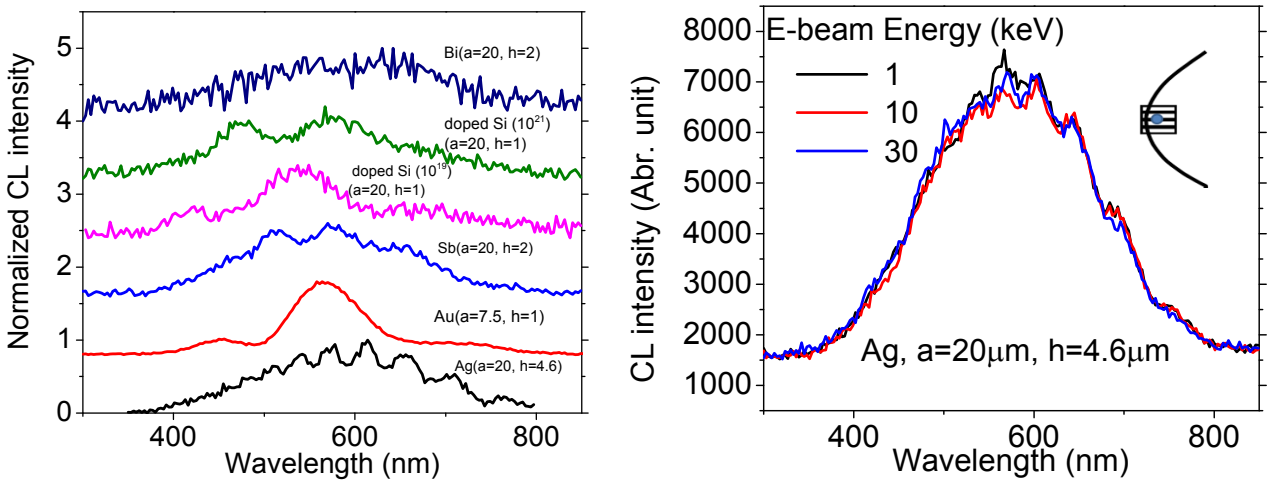

Fig. 5: (left). CL for different other materials including Au, Ag, Sb, Bi, and doped Si. The flat featureless beam-off baseline amounting to about 10% of the signal has been subtracted and the resulting spectra normalized. (right). Raw CL spectra for silver gratings with different e-beam energy. The inset shows the grating-orientation and a schematic outline of the parabolic collection mirror, while the blue dot indicates the location of the e-beam spot.

Fig. 6 (left) presents normalized CL spectra as a function of z. Spectra are offset vertically by 0.4 for clarity. The fringe visibility clearly has a strong z dependence. We observe that the visibility has double peak. The integrated intensity also follows the same trend as visibility. These effects are partly and qualitatively explained by Fig. 3 (right): A minimum fringe visibility might be expected to occur at the focus of the collection optic because fewer grating bars contribute to the collected light at that position.

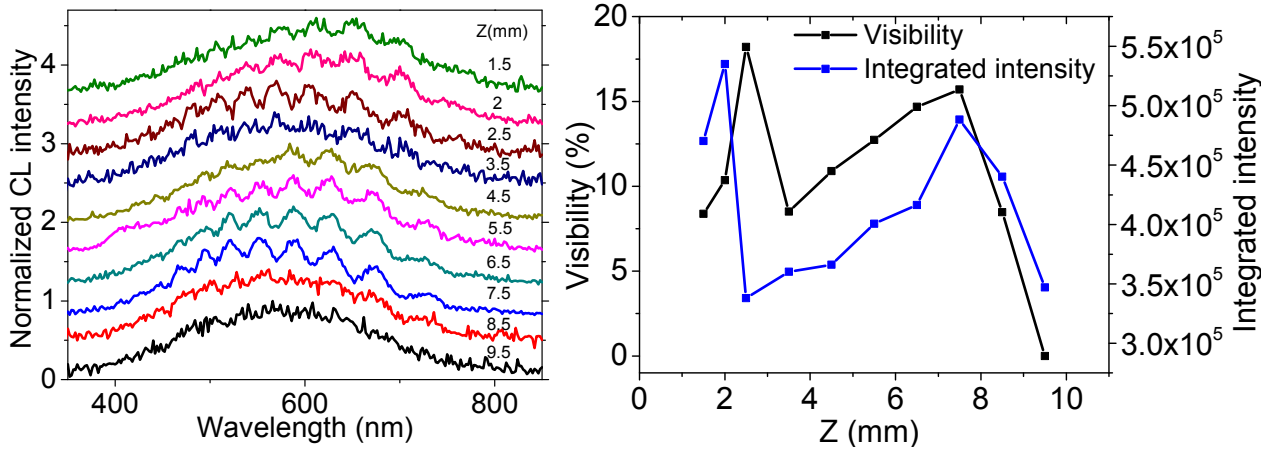

Fig. 6: (left) Normalized CL spectra for different distances z between sample and collection optic. (right) Dependence of fringe visibility and integrated intensity on z.

Fig. 7 (left) presents CL spectra when the excitation spot is separated from the FIB gold grating by varying distances up to 1 mm. The grating has a = 1 μm, h = 100 nm, and is oriented parallel to the collection axis. There is little dependence in spectral intensity or shape on e-beam distance from the grating. Since SPP propagation lengths on gold are not more than about 10 microns even at the longest visible wavelengths, there appears to be no contribution from SPPs, in contrast to prior studies[1,2,3]. Very far from the grating, on the smooth gold surface, no band is seen of above the usual beam-off baseline of ~1500 counts. Fig. 7 (right) confirms the importance of a grating to the observation of an emission band. Presented are spectra from smooth Ag, Au, and Si surfaces. The usual emission band is nearly absent when there is no

grating, so that only the usual beam-off baseline of ~1500 counts is observed. This indicates a strong role of the grating in outcoupling the CL signal or in its physical generation mechanism.

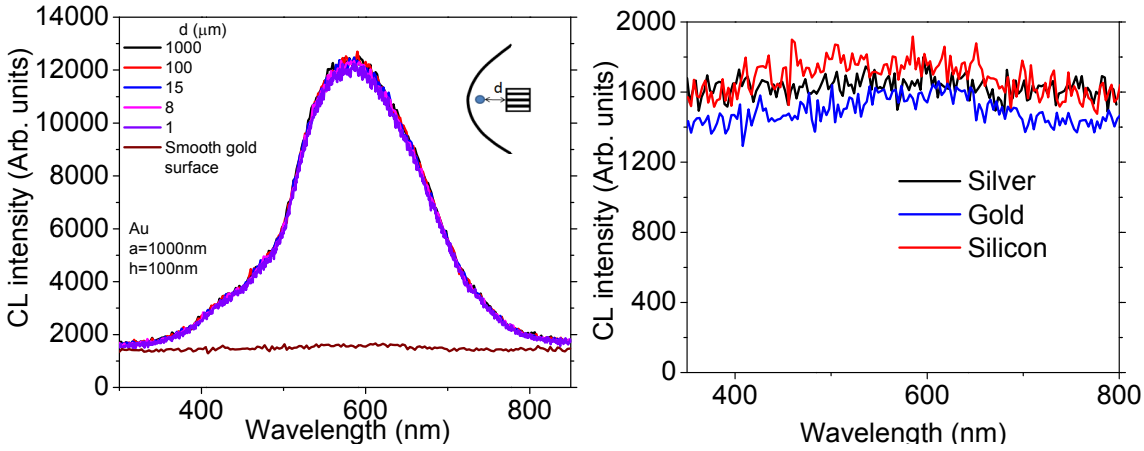

Fig. 7: (left) CL spectra for electron beam excitation spot away from the FIB gratings (a = 1 micron, h = 100 nm). The spectrum for the smooth gold surface was taken on a portion of the same wafer that was broken off from the part that contains the FIB grating. (right) Weak, nearly flat, CL spectra from smooth unstructured Ag, Au and Si surfaces.

Fig. 8 (left) shows SEM image of the surface of a single-crystal sample of copper. The roughness on the surface can be estimated to be at least 1 micron from the features from the SEM image. Fig. 8 (right) presents its CL spectrum, which has the usual broad peak around 600 nm, though rather weaker than in the case of the grating samples. When the Cu sample is polished using a final grit size 0.3 micron, so that roughness is no longer evident in the electron micrograph, the usual CL band is significantly reduced. These results confirm the Fig. 7 observation that surface corrugation is a necessary condition to observe the 600 nm band. These results also confirm that grating period does not influence the envelope of the CL spectrum, and it need not even be periodic, since here the corrugation is random. However, periodic gratings do seem more effective: After the final polish, the Cu sample has remaining random roughness of order 300 nm and the signal is almost gone, but small, periodic, FIB-milled gratings of only 100 nm amplitude give strong signals (Fig. 7, left).

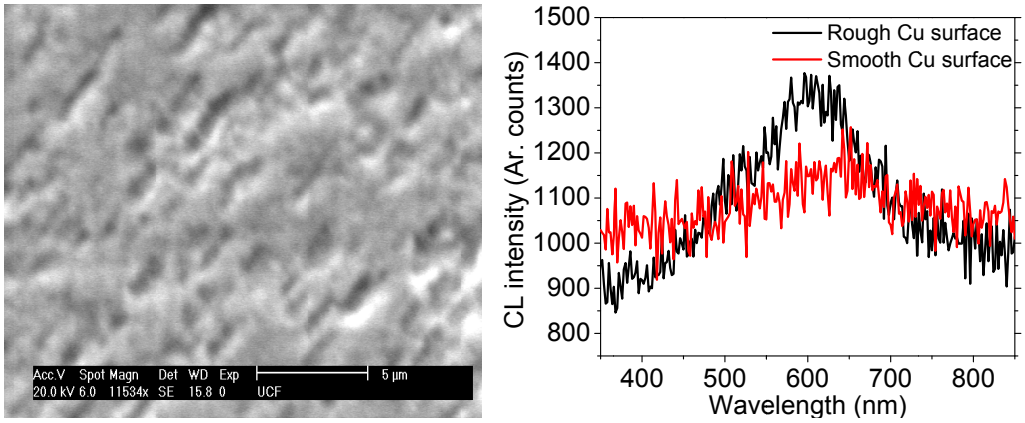

Fig. 8: (left) SEM image of the surface of a single-crystal of copper. (right) CL spectrum from the Cu surface before and after fine polishing with 0.3 micron grit.

Fig. 9 (left) presents CL spectra for a 20-micron-period Ag grating with 4.6 micron amplitude as a function of filament heater current. The electron beam current might be expected to be proportional to the square of the heater current from considerations of Joule heating. Fig. 9 (right) plots the CL peak intensity with the ~1500 count baseline subtracted. The CL band intensity does appear to increase as the square of the heater current but with a constant offset. Fig. 10 (left)

presents the peak wavelength and band width, calculated by fitting a Gaussian to the background-subtracted normalized spectra at different filament currents. There is ~2% blue shift with increasing filament current; however there is no significant change in bandwidth with current.

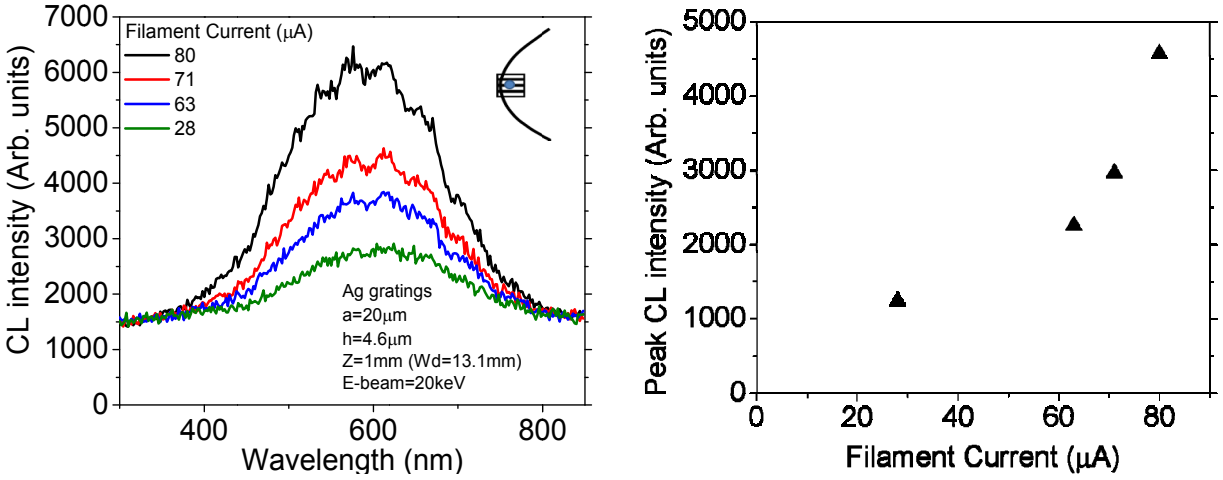

Fig. 9: (left) CL spectra for varying filament current on an Ag grating. (right) CL intensity as a function of filament heating current.

Fig. 10 (right) presents CL spectra obtained on a tilted 20-micron-period silver grating with grating amplitude 4.6 microns. This 0.5 cm × 0.5 cm grating pattern is surrounded by smooth surface. The sample is tilted so that the electron beam is incident at an angle of 26.1 degrees. The inset in Fig. 10 shows the tilted sample, which is mounted at 26.1 degrees to the SEM stage. The electron beam is positioned at different distances from the top edge of the grating up to a maximum distance of 2 mm. The vertical position of the sample stage is fixed for this experiment so the distance between the mirror and the sample surface varies by a maximum of 2Sin[29.1] mm = 1 mm. Unlike the case of a horizontal sample (Fig. 7), the CL intensity and fringe visibility both decrease strongly as the beam is moved away from the edge of the grating. This may be explained entirely in terms of geometrical factors, like collection efficiency and focus (Fig. 3, right).

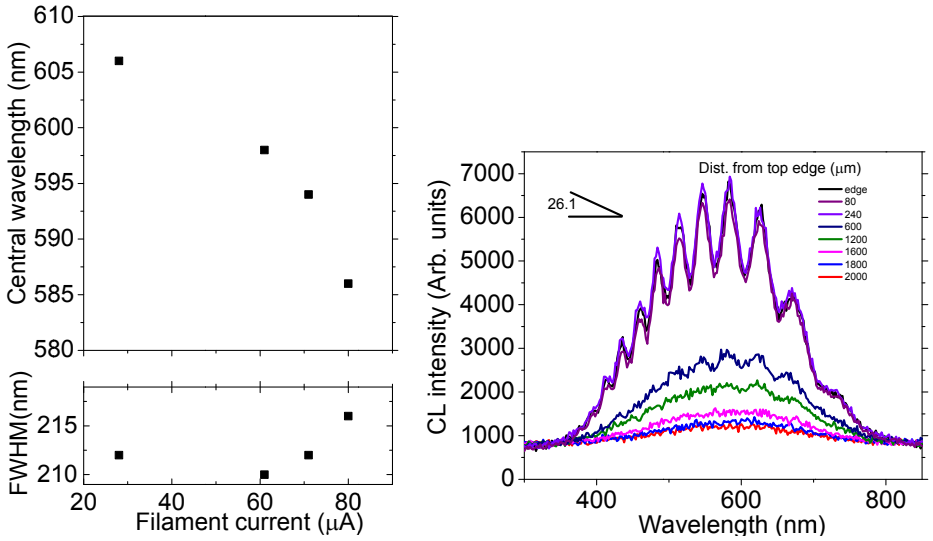

Fig. 10: (left) Central wavelength and band width versus filament current. (right) CL intensity for electron beam incident at an angle of 26.1 degrees on 20-micron-period silver gratings with grating amplitude 4.6 microns. Different curves are for CL spectra excited at different electron-beam distance from the top edge of the grating.

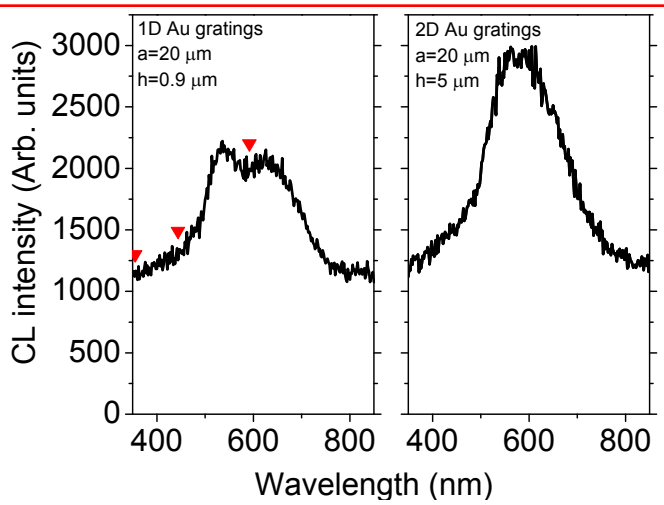

Fig. 11: (Left) CL spectrum from a 20-micron-period 1-dimensional grating (Au on ProLIFT) with grating amplitude of 0.9 microns. Red triangles indicated predicted interference peaks. (right) CL spectrum from a 20-micron-period 2-dimensional grating (Au on ProLIFT) with grating amplitude of 5 microns.

Fig. 11 (left) presents a CL spectrum from 1-dimensional grating formed by evaporating Au on ProLIFT with grating a 20-micron-period and an amplitude h = 0.9 microns. Modulation of the spectrum is in agreement with the positions indicated by red triangles using $\lambda = 2h/m$, where m is an integer. Fig. 11 (right) represents CL spectrum from 20-micron-period 2-dimensional gratings on ProLIFT with grating amplitude of 5 microns. The envelope of the spectrum for the 2-dimensional grating looks the same as that of the 1-dimensional gratings. A distinction that requires further investigation is that the 2D grating apparently does not give rise to strong modulation, regardless of the position z below the collection optic.

Fig. 12 presents CL spectra from FIB milled 0.5- and 1-micron-period gratings of 100 nm grating amplitude at temperatures 50 and 100^0 C. With increase in temperature, the CL intensity decreases in each case. Since e-beam induced hot-electron currents that travel 10s of microns to excite CL at gratings have already been inferred by our results, the temperature-induced decrease in CL intensity might be explained in a reduction of the electron mean-free-path due to temperature activated scattering.

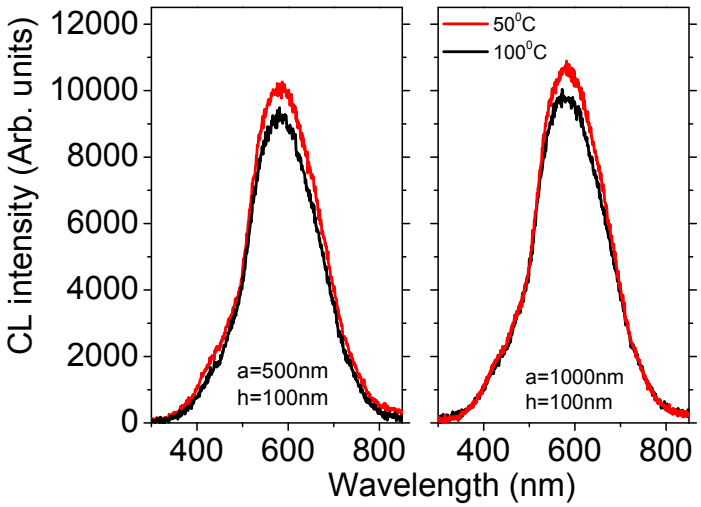

Fig. 10: Background subtracted CL spectra from (left) 500 nm-period (right) 1-micron-period grating at temperatures 50^0 C and 100^0 C. Grating amplitudes are both 100 nm.

5. SUMMARY

Cathodoluminescence spectroscopy on a variety of structured conducting surfaces reveal a broad band centered at ~600 nm that originates from sample areas more than three orders of magnitude larger than the excitation beam spot size. The material type of the surface or substrate is immaterial to the spectrum. Some surface corregation appears necessary to the generation of CL, and periodic patterns seem more efficient at generating signal than is random roughness, though the grating period is immaterial. The grating depth does have an effect on the spectrum, since interference fringes appear in the spectrum with the depth is at least 1 micron. These observations, together with theoretical considerations, invalidate previously proposed explanations for the origin of the signal.

6. ACKNOWLEDGEMENTS

This work is supported by AFOSR grant number FA 95501010030, Gernot Pomrenke, Program Manager.

REFERENCES

[1] Bashevoy, M. V., Jonsson, F., Krasavin, V., Zheludev, N. I., Chen, Y., and Stockman, M. I., "Generation of traveling surface plasmon waves by free-electron impact.," Nano letters 6(6), 1113-1115 (2006).
[2] Bashevoy, M. V., Jonsson, F., Macdonald, K. F., Chen, Y., and Zheludev, N. I., "Hyperspectral imaging of plasmonic nanostructures with nanoscale resolution.," Optics express 15(18), 11313-11320 (2007).
[3] Wijngaarden J. T. van, Verhagen, E., and Polman, A., Ross, C. E., H. J. Lezec,b and Atwater, H. A., "Direct imaging of propagation and damping of near-resonance surface plasmon polaritons using cathodoluminescence spectroscopy," Applied Physics Letters 88(22), 221111(2006).
[4] Peale, R. E., Lopatiuk, O., Cleary, J., Santos, S., Henderson, J., Clark, D., Chernyak, L., Winningham, T. A., Del Barco, E., Heinrich, H., and Buchwald W. R., "Propagation of high-frequency surface plasmons on gold," Journal of the Optical Society of America B 25(10), 1708 (2008).
[5] García de Abajo, F. J., "Optical excitations in electron microscopy," Reviews of Modern Physics 82(1), 209-275 (2010).
[6] Barnes, W. L., Dereux, A., and Ebbesen, T. W., "Subwavelength optics," Nature 424, 824-830 (2003).
[7] Smith, N. V., "Inverse photoemission," Reports on Progress in Physics 51(9), 1227-1294 (1988).
[8] Kagami, S., Minoda, H., Yamamoto, N., "STM light emission from Si(1 1 1)$\sqrt{3}\times\sqrt{3}$ -Ag surface." Surface Science, 493, 78(2001)
[9] Landau, L. D. and Lifshitz, E. M., [The Classical Theory of Fields, 4th Ed], Elsevier Butterworth Heinemann, New York, Section 70 (1975).
[10] Frank, I., "Transition radiation and optical properties of matter," Soviet Physics Uspekhi 8(5), 1227-1294 (1966).
[11]Nath, J., Schwarz, C., Lin, Y., Smith, E., Peale, R. E., Chernyak, L., Buchwald, W. R., Lee, J., "Cathodoluminescence study of silver and gold lamellar gratings," Proc. SPIE8031, 101 (2011).